

This is the accepted manuscript made available via CHORUS. The article has been published as:

# Nonperturbative effects and indirect exchange interaction between quantum impurities on metallic (111) surfaces

A. Allerdtd, R. Žitko, and A. E. Feiguin

Phys. Rev. B **95**, 235416 — Published 9 June 2017

DOI: [10.1103/PhysRevB.95.235416](https://doi.org/10.1103/PhysRevB.95.235416)

# Non-perturbative effects and indirect exchange interaction between quantum impurities on metallic (111) surfaces

A. Allerdt,<sup>1</sup> R. Žitko,<sup>2</sup> and A. E. Feiguin<sup>1</sup>

<sup>1</sup>*Department of Physics, Northeastern University, Boston, Massachusetts 02115, USA*

<sup>2</sup>*Jožef Stefan Institute, Jamova 39, SI-1000 Ljubljana, Slovenia*

The (111) surface of noble metals is usually treated as an isolated two dimensional (2D) triangular lattice completely decoupled from the bulk. However, unlike in topological insulators, bulk bands also cross the Fermi level. We here introduce an effective tight-binding model that accurately reproduces results from first principles calculations, accounting for both surface and bulk states. We numerically solve the many-body problem of two quantum impurities sitting on the surface by means of the density matrix renormalization group. By performing simulations in a star geometry, we are able to study the non-perturbative problem in the thermodynamic limit with machine precision accuracy. We find that there is a non-trivial competition between Kondo and RKKY physics and as a consequence, ferromagnetism is never developed, except at short distances. The bulk introduces a variation in the period of the RKKY interactions, and therefore the problem departs considerably from the simpler 2D case. In addition, screening and the magnitude of the effective indirect exchange are enhanced by the contributions from the bulk states.

PACS numbers: 73.23.Hk, 72.15.Qm, 73.63.Kv

## I. INTRODUCTION

Nano-structures assembled on crystal surfaces through single-atom manipulation with a scanning tunneling microscope (STM) can serve as model systems for studying magnetism with atomic real-space resolution as well as excellent energy resolution.<sup>1–3</sup> This technique can, for example, uncover spatial profiles of magnetic excitations in artificial one-dimensional spin chains<sup>4–7</sup>. The surface not only supports the spin centres, but also plays a crucial role in stabilizing magnetic order<sup>8–11</sup>. The impurities are coupled through exchange interactions of different physical origins, either direct exchange for nearest-neighbor adsorption sites or indirect substrate-mediated coupling that asymptotically decay as a power-law with increasing separation between the impurities (Ruderman-Kittel-Kasuya-Yosida or RKKY interaction)<sup>12–14</sup>. The indirect exchange coupling depends on the nature of the substrate states involved: in addition to bulk states, some commonly used noble metal substrates, such as Cu(111), also have a band of surface states crossing the Fermi level<sup>15,16</sup>. The existence of surface states in metals was first predicted in 1930s by I. Tamm and W. Shockley<sup>17–19</sup>. Originating from the atomic levels, it was shown how these states appear when the boundary of the crystal is formed. The momentum-resolved electronic structure on the surface of copper<sup>20</sup> and other noble metals<sup>21</sup> has been studied using angle-resolved photoemission spectroscopy<sup>22</sup>. More recently, the dispersion of surface states has also been studied in Cu and Ag using an STM<sup>23</sup>. First principles and analytic calculations have predicted long-ranged oscillatory adsorbate-adsorbate interactions mediated by these surface states<sup>24–26</sup>. Their findings are consistent with a 2D RKKY interaction that decays asymptotically as  $\sim 1/R^2$ .

In the presence of both bulk and surface states, as is commonly the case, the distance dependence of the exchange coupling at intermediate distances, which are also physically the most relevant, is non-trivial. Moreover, at very short inter-impurity separation the atomistic details become important

and lead to significant directional anisotropy. In addition, for strong impurity-substrate couplings the effective impurity-impurity exchange coupling can no longer be reliably determined through low-order perturbation theory estimates as in the simple RKKY picture. This approach become particularly troublesome in situations where non-perturbative effects, such as the Kondo screening<sup>27–29</sup>, are also significant. For instance, in a recent study of Fe atoms on Cu(111) surface, their mutual interactions were measured with spin-resolved STM<sup>5</sup> and the data was interpreted in terms of an Ising model which does not include any many-body effects. In such cases, reliable non-perturbative techniques are required for an unbiased analysis. Such methods, based on the density matrix renormalization group (DMRG) group, have recently been developed<sup>30,31</sup>. They allow one to study the full many-body problem with a realistic description of the band structure obtained from atomistic first principles calculations. The resulting tight-binding-model description of the substrate can be *exactly* mapped onto a 1D representation suitable for the DMRG calculations. This approach is numerically exact and correctly describes correlation effects and, in particular, the Kondo singlet formation.

Many of the early STM experiments on single magnetic adsorbates exhibiting a Kondo resonance were performed on the (111) surfaces of noble metals such as Cu and Ag that host surface-state bands<sup>32–34</sup>. Since both surface-state and bulk conduction band electrons hybridize with the adsorbate, the question of which one plays the dominant role has been widely debated<sup>35,36,38,39</sup>. A number of experiments suggested a more important role of the bulk states in the formation of Kondo state even on (111) surfaces<sup>34–36,40</sup>: for example, the resonance width is not affected when the adatom is moved close to the step edges where the surface-state electron local density of states is modulated by a standing wave pattern<sup>34</sup>. On the other hand, the quantum mirage experiments<sup>33</sup> clearly demonstrate that the Kondo resonance is projected from one focus to the other in an elliptical quantum corral, which necessarily involves the surface-state electrons. Recently, Kondo physics has also been explored on the Si(111)- $\sqrt{3} \times \sqrt{3}$ Ag

substrate, which is a semiconductor with a metallic surface: a long decay length of the Kondo resonance has been observed<sup>41</sup>.

The usual treatment to derive an effective exchange interaction between the localized moments involves second-order perturbation theory. The result can be summarized as:

$$J_{RKKY}(\mathbf{R}) = J_K^2 \chi(\mathbf{R}),$$

where  $\chi(\mathbf{R})$  is the Fourier transform of the non-interacting static susceptibility, or Lindhard function, and  $J_K$  is the Kondo coupling between the impurities and the conduction electrons. In this paper, we numerically study the adatom-adatom interactions on a (111) surface, with metallic bulk and surface states, non-perturbatively, and with full real-space resolution. We consider quantum spins  $S = 1/2$  and we show important departures from the conventional perturbative RKKY interpretation. In particular, long-ranged interactions are absent because of the formation of separate Kondo-singlet states<sup>31</sup>.

The paper is structured as follows: In Section II we introduce the model and methods, emphasizing on a new computational development that is introduced in this context for the first time. We describe our results in Section III, and we finally close with a discussion.

## II. MODEL AND METHOD

### A. Band Structure

Unlike the boundary states in topological insulators, the Shockley surface states are metallic and coexist near the Fermi level with other bulk bands that are also partially filled. We begin our discussion with a three band tight binding model on a semi-infinite chain. We will then be able to extend the idea to three dimensions, where each site on the chain will become a triangular plane arranged to form an FCC lattice. The bands are described by hopping parameters  $t_1, t_2, t_3$  and  $t_p$  as shown in Fig. 1. This model will host a surface, or edge state on the topmost  $A$  sites as expected from the one-dimensional Peierls chain with hoppings  $t_1 - t_2$ . In addition, due to the inclusion of the  $B$  sites, we will obtain an additional metallic band. It is worth noting that this model is not built from first principles considerations or the chemistry of copper. Instead we are proposing a phenomenological approach that reproduces not only the band structure, but also differentiates between surface and bulk in the same spirit as topological insulators. The goal is to build a 3-dimensional model with metallic surface and bulk bands. For an alternate method of obtaining Shockley surface states see Ref. 43. We begin by following the method prescribed by Pershoguba and Yakovenko in Ref. 42 to find the energy of this state by extending the treatment to a three-band problem. The Hamiltonian for a translational invariant chain in momentum space can be represented by the matrix:

$$H = \begin{pmatrix} \epsilon_A & 0 & t_1 + t_2 e^{ik} \\ 0 & \epsilon_B + t_3 \cos(k) & t_p \\ t_1 + t_2 e^{-ik} & t_p & \epsilon_C \end{pmatrix} \quad (1)$$

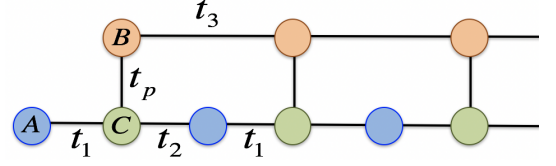


FIG. 1: Diagram of the chain with sites A, B, and C and hoppings  $t_1, t_2, t_3$  and  $t_p$ .

One key feature of this Hamiltonian that allows us to find an explicit expression for the surface state, is that the  $A$  sites are not directly coupled to the  $B$  sites. The Schrodinger equation can be expressed as:

$$V\Psi(z) + (U - E)\Psi(z + 1) + V^\dagger\Psi(z + 2) = 0 \quad (2)$$

where we introduce the spinor

$$\Psi(z) = \begin{pmatrix} \psi_A(z) \\ \psi_B(z) \\ \psi_C(z) \end{pmatrix} \quad (3)$$

Here  $z \geq 1$  labels the unit cell along the chain direction and the wave functions  $\psi$  sit on sites  $A, B$ , or  $C$ , which represent three orbitals of a copper atom that could originate from hybridizations of  $s, p$ , and  $d$  atomic orbitals. In this expression we use the matrices  $U$  and  $V$  defined as:

$$U = \begin{pmatrix} \epsilon_A & 0 & t_1 \\ 0 & \epsilon_B & t_p \\ t_1 & t_p & \epsilon_C \end{pmatrix} \quad V = \begin{pmatrix} 0 & 0 & t_2 \\ 0 & t_3 & 0 \\ 0 & 0 & 0 \end{pmatrix}. \quad (4)$$

Following Ref. 42, we introduce the generating function

$$G(q) = \sum_{z=1}^{\infty} q^{z-1} \Psi(z), \quad (5)$$

that can be re-written as

$$G(q) = [q^2 V + q(U - E) + V^\dagger]^{-1} \Psi(1), \quad (6)$$

where we have used the boundary condition

$$(U - E)\Psi(1) + V^\dagger\Psi(2) = 0 \quad (7)$$

Yakovenko *et al.*<sup>42</sup> showed that for a given energy  $E$ , a surface state exists if all poles of  $G(q)$  have magnitude greater than one. For our 1D chain, this state exists at  $E = \epsilon_A$ , just as the two-orbital case, under the condition  $|t_2| > |t_1|$ . Also note that the surface state *only* exists on the  $A$  sites.

This same procedure can be generalized to a three-dimensional structure (an FCC crystal in our case). The hoppings now acquire an in plane  $(p_x, p_y)$  dependence. The in-plane hoppings are denoted as  $t_A, t_B$  and  $t_C$ . The Hamiltonian of the bulk is now

$$H = \begin{pmatrix} \epsilon_A + h_A & 0 & t(\vec{p}, k) \\ 0 & \epsilon_B + h_B + t_3(\vec{p}, k) & t_p \\ t^*(\vec{p}, k) & t_p & \epsilon_C + h_C \end{pmatrix}. \quad (8)$$

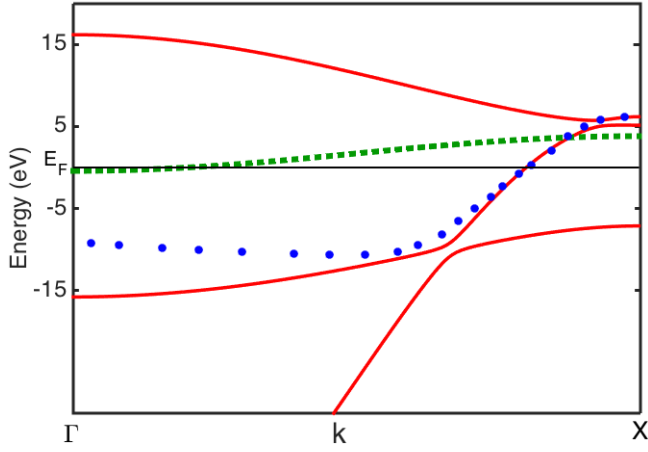


FIG. 2: Band structure of our model copper system as obtained with the method described in the text. Red lines show bulk bands while the green line is the surface state. Blue points are theoretical values taken from Ref. 44

where,

$$\begin{aligned}
 h_\lambda &= t_\lambda \left( 2\cos(p_x) + 4\cos(p_x/2)\cos(\sqrt{3}p_y/2) \right) \\
 t(\vec{p}, k) &= t_1 + t_2 e^{-i\sqrt{2/3}k} \left( e^{-i\sqrt{3}p_y/3} + 2e^{i\sqrt{3}p_y/6}\cos(p_x/2) \right) \\
 t_3(\vec{p}, k) &= t_3 \left( 2\cos(\sqrt{2/3}k + \sqrt{3}p_y/3) \right. \\
 &\quad \left. + 4\cos(p_x/2)\cos(\sqrt{2/3}k - \sqrt{3}p_y/6) \right), \quad (9)
 \end{aligned}$$

where the subindex  $\lambda$  can represent any one of the three orbitals  $A, B, C$ . Following the same reasoning as before for a chain, it can be found that the energy of the surface state is given by

$$E = \epsilon_A + t_A \left( 2\cos(p_x) + 4\cos(p_x/2)\cos(\sqrt{3}p_y/2) \right), \quad (10)$$

which is the same as the dispersion of the triangular lattice.

The parameters in the model are adjusted to give a good description matching both first principles calculations and experiments of the copper (111) surface. First, we fix  $t_A$  and  $\epsilon_A$  to fit the surface state energy at the  $L$ -point and its Fermi momentum. This state has a binding energy<sup>22</sup> of about  $-0.4\text{eV}$  and Fermi vector  $k_f \approx 0.2\text{\AA}^{-1}$ . The remaining parameters (shown in Table I) are used to fit the bands near the Fermi level along the  $\Gamma - X$  line (Fig. 2). The theoretical data shown in Fig. 2 is taken from Ref. 44. Although one could argue that this is to some extent a toy model, we are able to obtain the correct surface band energy near the  $\Gamma$  and  $L$  points, we match the Fermi momentum of the surface band, fit the bulk bands along  $\Gamma - X$  near the Fermi energy, all while preserving the symmetry of an FCC lattice. The power of this model also lies in being able to study the effects of bulk bands on surface physics. Fig. 2 shows the resulting bands, accompanied by the local density of states in Fig. 3. Notice the local density of states (LDOS) of the surface has a form very similar to that of a 2D triangular lattice with some contributions from the bulk bands, as expected.

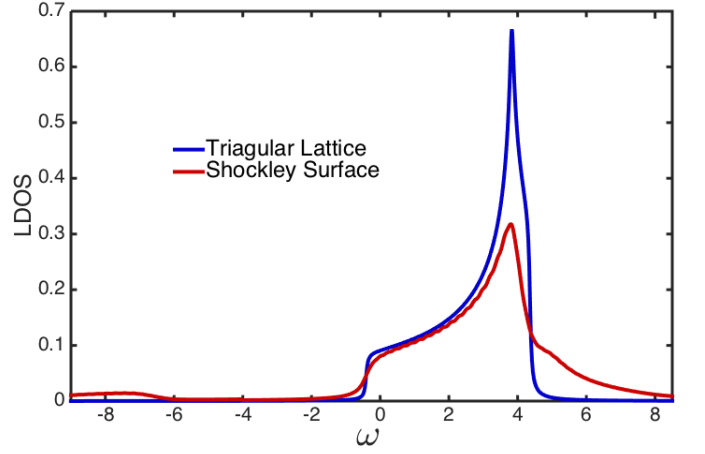


FIG. 3: LDOS for a site on the Shockley surface as well as a 2D triangular lattice with the same bandwidth, where zero energy corresponds to the Fermi level. The 2D results are in the thermodynamic limit, while the Shockley data corresponds to 500 poles. Bulk states have very small weight below the Fermi level.

$t_1$	$t_2$	$t_3$	$t_p$	$t_A$	$t_B$	$t_C$	$\epsilon_A$	$\epsilon_B$	$\epsilon_C$
1.0	5.0	-4.0	-1.0	-0.53	-4.0	0.8	2.77	-10.0	-4.2

TABLE I: Model parameters (in eV) used in calculations throughout the paper. Note that small changes in the parameters do not induce qualitative changes in the results.

## B. Numerical approach

Having obtained an accurate representation of the bulk and surface bands, we now introduce the magnetic atoms as two  $S = 1/2$  Kondo impurities at positions  $r_1$  and  $r_2$ , connected to the surface through the many-body exchange interaction:

$$V = J_K \left( \vec{S}_1 \cdot \vec{s}_{r_1} + \vec{S}_2 \cdot \vec{s}_{r_2} \right), \quad (11)$$

where  $J_K$  is the Kondo coupling constant.

In order to make the problem numerically tractable, we employ the so-called block Lanczos method recently introduced in this context by two of the authors<sup>31,45</sup>. This approach is inspired by Wilson's original formulation of the numerical renormalization group<sup>46</sup>, but accounting for the lattice structure. It enables one to study quantum impurity problems in real space and in arbitrary dimensions with the density matrix renormalization group method (DMRG)<sup>47,48</sup>. This is done through a unitary transformation to a basis where the non-interacting band Hamiltonian has block diagonal form. As described in detail in Refs. 31 and 45, this is equivalent to a block Lanczos iteration, where the recursion is started from seed states corresponding to electrons sitting at the positions of the impurities. The resulting matrix can be re-interpreted as a single-particle Hamiltonian on a ladder geometry.

The Lanczos transformation is carried out by taking  $A$  sites on the surface at the impurity positions to be the seed states. Since we are considering impurities on the surface of a 3D system, a ladder of length  $L$  will contain contributions from

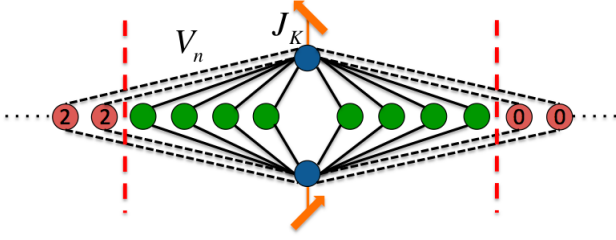


FIG. 4: A representation of the star geometry. The blue circles represent sites in real space or the “seed” states in the Lanczos transformation. The new bath sites are shown in green and red. The green represent the relevant sites while the red are discarded indicated by the dashed red line where the system is effectively truncated. The red sites are either doubly occupied (“2”) or empty (“0”). The orange arrows correspond to Kondo spin-1/2 impurities coupled via  $J_K$ .

both surface and bulk states, with the large majority of these states having larger weight in the bulk. In order to reach the desired extremely large systems, we introduce an improvement to the aforementioned method. It was shown that transforming from a ladder to a star geometry results in lower ground state entanglement than the ladder geometry<sup>49</sup>, making it ideal for DMRG. A pictorial representation of the new geometry<sup>37</sup> for the two impurity problem is shown in Fig. 4. This mapping corresponds to a second unitary transformation on top of the ladder geometry. The seed states remain unchanged and are now coupled to the bath states with on-site energy  $\epsilon_n$  via new hoppings  $V_n$ . The new system is very advantageous in our case since the surface states are very weakly coupled to the bulk states at high and low energies. Fig. 5(a) shows the occupation of the orbitals as a function of energy. Orbitals below(above) a certain energy have occupation exactly equal to 2(0), and can be discarded without losing any physics. This allows us to carry out simulations in extremely large systems of the order of  $800^3$  lattice sites keeping of the order of 200 orbitals! We find that the results are absolutely free of finite size effects and therefore they represent the thermodynamic limit for all practical purposes. In all our simulations, we use 1000 DMRG states, which yield results with machine precision accuracy in both energy and correlations.

To make this more evident, we place the orbitals in a line in increasing order by their local orbital energy as shown in Fig. 4 and we calculate the entanglement entropy between the low energy and high energy states. This quantity is plotted as a function of the energy where we make the cut in Fig. 5(b). The arrow in the figure shows where the impurities are placed in the DMRG simulation. Clearly, the double occupied and empty orbitals at the edges of the spectrum are completely disentangled from the rest of the system. More interestingly, most of the entanglement is contained in the energy window corresponding to the surface band  $0 \leq \epsilon \leq 5$ , with a small but significant residual entropy in the bulk bands in the range  $-10 \leq \epsilon \leq 0$ .

To further demonstrate that truncating the star geometry has no effect on the physical properties, the spin correlations as a function of number of bath sites kept is shown in Fig. 6 for the same distance and value of  $J_K$  used in Fig. 5. As the window

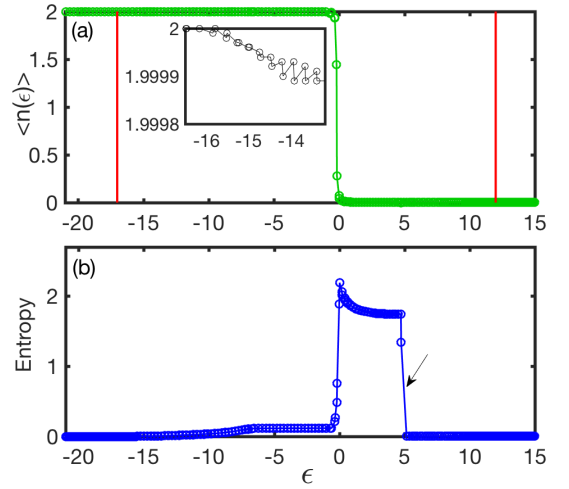


FIG. 5: (a) Orbital occupation as a function of on-site energy. Red vertical lines indicate where the system is truncated. Inset shows a zoomed in region near the cut-off energy; only sites with occupation exactly 0 or 2 are discarded. Parameters are  $J_K = 1$  and  $R = 4$ . (b) Block entanglement entropy between left and right half of the system, when orbitals are placed along a chain in increasing order by their local energy. In the DMRG simulation, the impurities are located at the position indicated by the arrow.

size is increased towards the cut-off, convergence to the given value is clear. Note that for small windows most of the bath sites are surface states, and extending the window reveals the effect of the higher energy bulk states.

### III. RESULTS

We first recall the expression for the Lindhard function:

$$\chi(\mathbf{r}_1, \mathbf{r}_2) = 2\text{Re} \sum \frac{\langle \mathbf{r}_1 | n \rangle \langle n | \mathbf{r}_2 \rangle \langle \mathbf{r}_2 | m \rangle \langle m | \mathbf{r}_1 \rangle}{E_n - E_m}, \quad (12)$$

where the sum is over the eigenstates  $n, m$  with energies  $E_n > E_F > E_m$ . The  $|\mathbf{r}_{1,2}\rangle$  are the single-particle states at positions  $\mathbf{r}_{1,2}$ . This function can be computed numerically for our systems, and compared to the non-perturbative results obtained by solving the many-body problem.

Results for spin-spin correlations as well as the perturbative result (Lindhard function) are shown in Fig. 7. We only display the  $z$  component of the spin since the problem is  $SU(2)$  symmetric. The particle number was adjusted to match the Fermi level in copper. For the triangular lattice, the filling is such that the Fermi level is at the same point as the surface band, i.e., we are in the low density regime. An interesting feature is that ferromagnetism is found on the Shockley surface at  $R = 1$ , consistent with the Lindhard function as well as the result in Ref. 8, where  $R$  is the impurity separation along the nearest neighbor direction in units of lattice spacing. Beyond  $R = 1$  however, the Kondo effect will dominate over ferromagnetism, whereas the perturbative results predict oscillations.



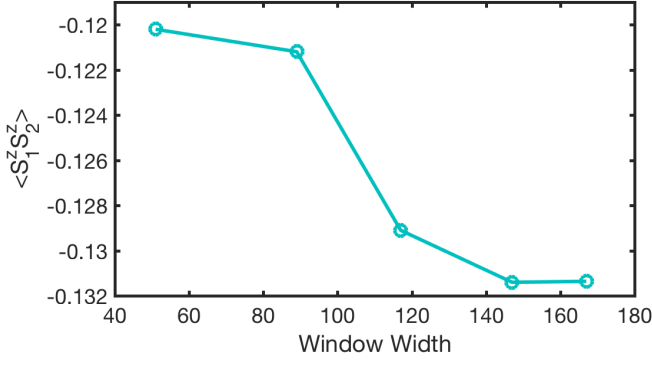


FIG. 6: Spin-spin correlations as a function of window size or number of bath sites with the same parameters used in Fig. 5.

In contrast, on the triangular lattice we find that all correlations are anti-ferromagnetic regardless of the value of  $J_K$ . At even weaker couplings, the impurities transition into a free moment regime which is attributed to the very low carrier density. When this occurs, our correlations acquire the value  $\langle S_1^z S_2^z \rangle = -1/4$ , are independent of impurity separation, and the magnetic moments are completely decoupled from the conduction electrons (and each other) resulting in a 4-fold degenerate ground state with spins pointing in either direction. Since we are enforcing spin conservation and  $S_{\text{Tot}}^z = 0$ , the impurities are always anti-parallel and correlations can only assume the value  $-1/4$ . This is in sharp contrast to the predicted power law decay. As the coupling is increased to  $2eV$ , the spins form their own Kondo clouds after a separation of just a few lattice spacings, signaled by zero correlations. In reality, correlations at these distances are of the order of  $10^{-4}$  and still preserve the  $SU(2)$  structure of a finite RKKY interaction, but as we shall see below, this state is very close energetically to two independent Kondo singlets. In this regime, both staggered and uniform magnetic susceptibilities are practically the same, and equal to the single impurity case.

Calculations were also conducted with increased filling on the triangular lattice, and our results are qualitatively the same, *i.e.*, there is a competition between anti-ferromagnetism and Kondo, with ferromagnetism completely absent. This is contrasting to the square lattice<sup>31</sup> and graphene<sup>50</sup> where some ferromagnetism is found at half filling, and it might be due to the non-bipartite nature of the triangular lattice.

There is a striking difference in the correlations on the Shockley surface as a function of  $J_K$ . At smaller values of the coupling  $J_K$ , correlations for the Shockley surface and the triangular lattice differ noticeably, but as the interaction is increased, they start resembling each other with the former having a slight increase in the screening due to the contributions from the bulk states. Not only is there an increase in Kondo screening, but there is a significant change in the wavelength of oscillation. This change in wavelength is also seen in the Lindhard function, but it is not as dramatic as in the many-body case. We attribute these effects to the influence of the bulk. The periods of the oscillations are similar to the periods of the Lindhard function, except at short distances where the impurities are tending toward free moments, again due to

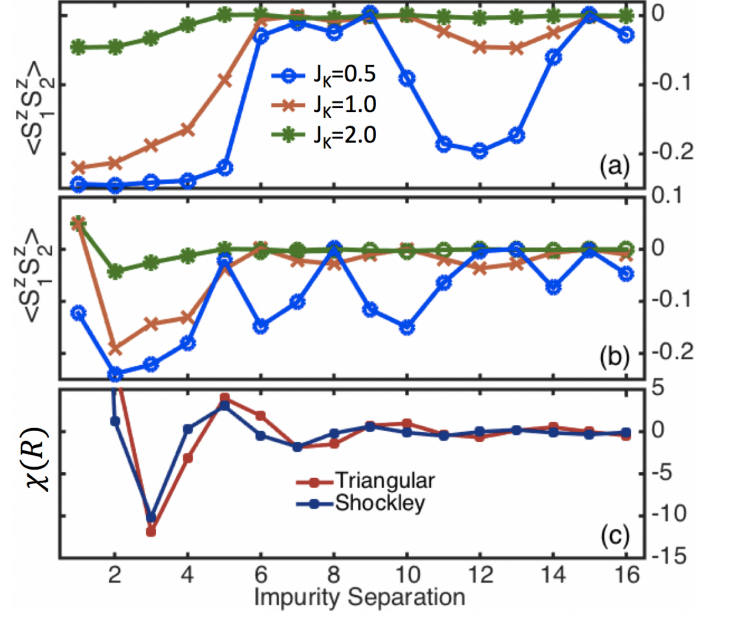


FIG. 7: Spin-spin correlations as a function of the impurity separation for (a) triangular lattice and (b) 2D Shockley surface of a (111) metal. (c) Lindhard function for the corresponding lattices. All plots are along the nearest neighbor direction, and the units of the coupling,  $J_K$ , are in  $eV$ .

the very low density in the surface band. Remarkably, at very short distances the correlations actually acquire the opposite sign! For larger  $J_K$ , and  $R = 1$ , the Lindhard function correctly predicts the ferromagnetic interaction for the Shockley case. This behavior is not seen in systems where there is only one band present at the Fermi level.

In order to understand the competition between Kondo and RKKY exchange we calculate the energy gain after the Kondo coupling  $J_K$  is turned on:

$$\Delta = E_0(J_K) - E_0(J_K = 0).$$

Results for this quantity as a function of the inter-impurity distance are shown in Fig. 8 for  $J_K = 1$ . In the absence of Kondo, this quantity is the characteristic RKKY energy scale  $E_{\text{RKKY}}$ . In addition, we also indicate the energy gain for two impurities very far apart (40 lattice sites), which should correspond to the characteristic energy scale for two independent Kondo singlets  $\Delta = 2E_K$ . Clearly, at distances  $R = 6, 10, 15$ , the impurities are very close in energy to two independent Kondo states, as also observed in the correlations.

It is possible to define a distance dependent Kondo energy  $E_K(R)$ . For this purpose, we introduce an external ferromagnetic interaction between the impurities:

$$H_{\text{FM}} = -J' \vec{S}_1 \cdot \vec{S}_2.$$

The effect of this term is to oppose the anti-ferromagnetic RKKY exchange. We expect the RKKY correlations to be completely destroyed at a critical value of  $J' = J'_{\text{crit}}$ . In that case, the impurities will form two independent Kondo states. Therefore, the energy gain at  $J'_{\text{crit}}$  would be twice  $E_K$  for that

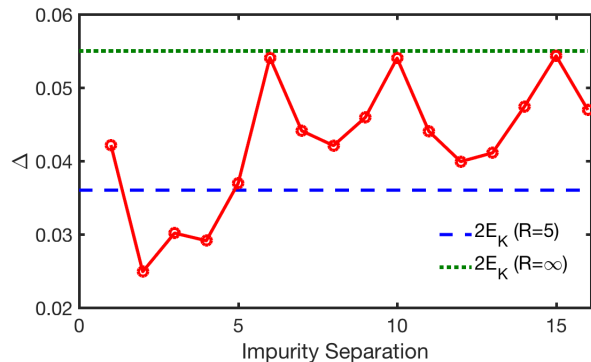


FIG. 8: Energy gain as a function of the inter-impurity distance as described in the text. The horizontal lines indicate the characteristic energy gains for forming two Kondo singlets  $\Delta = 2E_K$  at infinite distance apart and  $R = 5$ .

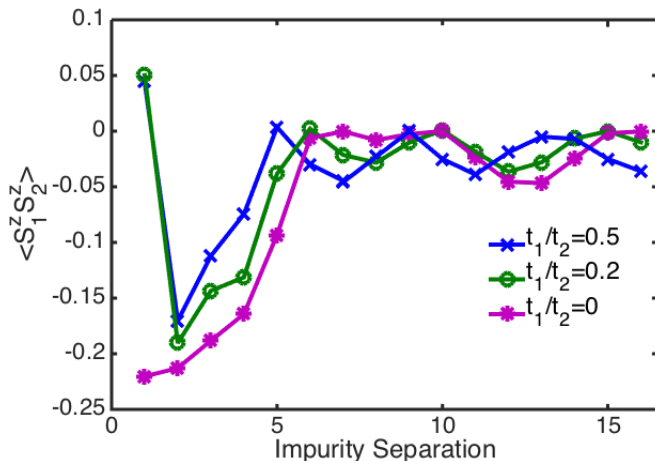


FIG. 9: Spin-spin correlations for different values of  $t_1/t_2$  for two spin  $S = 1/2$  impurities on the Shockley surface with  $J_K=1.0$ .

particular distance between the impurities. We have found that in most cases the system undergoes a first order transition from anti-ferromagnetic to ferromagnetic alignment, implying that the Kondo state is not stable. However, at distance  $R = 5$  there is a smooth crossover and we can compare both energy scales. As seen in the same Fig. 8, the RKKY state is slightly favorable. Even though  $E_{RKKY}$  is relatively large, it is likely that a small temperature will destroy the RKKY correlations due to the proximity to the Kondo state.

In addition to placing both impurities on the surface, calculations were done with one impurity in the bulk. It is found that correlations vanish after just one lattice space regardless of  $J_K$ , indicating that the surface states do not leak into the bulk: The impurity at the surface will couple mainly to the surface states (as indicated by the LDOS in Fig. 3 and the entanglement entropy in Fig. 5), and the impurity in the bulk will couple predominately to bulk states. As a consequence, the impurities will remain uncorrelated.

In Fig. 9 we show results obtained for different values of  $t_1/t_2$ . The case of  $t_1/t_2 = 0$  corresponds to a completely decoupled surface, *i.e.*, the triangular lattice. As  $t_1/t_2$  is in-

creased, the correlations behave differently. This can be seen in the change of period in the oscillations, as well as the sudden and dramatic change of sign of the correlations at distance  $R = 1$ . The surface bandwidth is parametrized by  $t_A$  in Eq. (9), and the contribution of this band to the Lindhard function remains unaffected. Therefore, this variation can only be attributed to the influence of the bulk states. Moreover, the values of  $t_1$  and  $t_2$  do not alter the Fermi surface of either surface or bulk bands; instead, they determine how the surface state decays into the bulk. This is telling us that the behavior of the RKKY interactions cannot be simply determined by the shape of the Fermi surface. In addition, when many-body effects are taken into consideration, competition with the Kondo effect becomes the dominant mechanism that determines the decay of the correlations.

It is very difficult to distinguish a particular power-law decay from our results (even on a log-scale). Even though the problem is three-dimensional, the physics is dominated by the surface. In addition, Kondo physics strongly affects the long-distance behavior of the correlations: after a certain distance the impurities will form two separate Kondo singlets and the RKKY correlations will vanish<sup>31</sup>.

#### IV. CONCLUSIONS

We have investigated the role of surface and bulk states on the effective indirect exchange between two quantum impurities. The metallic surface was modeled by means of a tight-binding Hamiltonian that reproduces the surface and bulk bands near the Fermi surface, as obtained from first principles calculations. The quantum many-body problem was then solved numerically by means of the DMRG method after mapping the non-interacting degrees of freedom to a star geometry. This approach allows us to study the problem in the thermodynamic limit, with machine precision accuracy. Most remarkably, ferromagnetism is completely absent, with the exception of impurities at distance  $R = 1$ , departing from the behavior observed in an isolated 2D triangular lattice. This effect clearly illustrates the subtle artifacts of perturbative approaches that are usually employed to guide experiments. We point out that at short distances it is very likely that direct exchange due to overlapping wave functions dominates the physics.

We found that the correlations extend to just one atomic layer into the bulk, and the main contributions originate from surface states. However, our results indicate that the bulk states introduce a change in the period of the oscillations of the RKKY interaction, and a non-trivial competition with Kondo physics. The RKKY interaction in these systems cannot be completely described in terms of an isolated 2D surface as also observed experimentally for the case of a single impurity in the Kondo regime<sup>34–36,40</sup>.

## Acknowledgments

We are grateful to C. F. Hirjibehedin for useful discussions. AA and AEF acknowledge the U.S. Department of Energy,

Office of Basic Energy Sciences, for support under grant DE-SC0014407. RŽ acknowledges the support of the Slovenian Research Agency (ARRS) under P1-0044 and J1-7259,

- <sup>1</sup> A. J. Heinrich, J. A. Gupta, C. P. Lutz, and D. M. Eigler, *Science* **306**, 466 (2004).
- <sup>2</sup> A. F. Otte, M. Ternes, S. Loth, C. P. Lutz, C. F. Hirjibehedin, and A. J. Heinrich, *Phys. Rev. Lett.* **103**, 107203 (2009).
- <sup>3</sup> A. Spinelli, M. P. Rebergen, and A. F. Otte, *Journal of Physics: Condensed Matter* **27**, 1 (2015).
- <sup>4</sup> C. F. Hirjibehedin, C. P. Lutz, and A. J. Heinrich, *Science* **312**, 1021 (2006).
- <sup>5</sup> A. A. Khajetoorians, J. Wiebe, B. Chilian, S. Lounis, S. Blügel, and R. Wiesendanger, *Nature Publishing Group* **8**, 497 (2012).
- <sup>6</sup> A. Spinelli, B. Bryant, F. Delgado, J. Fernández-Rossier, and A. F. Otte, *Nature Materials* **13**, 782 (2014).
- <sup>7</sup> R. Toskovic, R. van den Berg, A. Spinelli, I. S. Eliens, B. van den Toorn, B. Bryant, J. S. Caux, and A. F. Otte, *Nature Physics* **12**, 656 (2016).
- <sup>8</sup> V. S. Stepanyuk, L. Niebergall, R. C. Longo, W. Hergert, and P. Bruno, *Phys. Rev. B* **70**, 075414 (2004).
- <sup>9</sup> L. Zhou, J. Wiebe, S. Lounis, E. Vedmedenko, F. Meier, S. Blügel, P. H. Dederichs, and R. Wiesendanger, *Nat Phys* **6**, 187 (2010).
- <sup>10</sup> P. A. Ignatiev, N. N. Negulyaev, A. S. Smirnov, L. Niebergall, A. M. Saletsky, and V. S. Stepanyuk, *Phys. Rev. B* **80**, 165408 (2009).
- <sup>11</sup> P. Wahl, P. Simon, L. Diekhöner, V. S. Stepanyuk, P. Bruno, M. A. Schneider, and K. Kern, *Phys. Rev. Lett.* **98**, 056601 (2007).
- <sup>12</sup> K. Yosida, *Phys. Rev.* **106**, 893 (1957).
- <sup>13</sup> M. A. Ruderman and C. Kittel, *Phys. Rev.* **96**, 99 (1954).
- <sup>14</sup> T. Kasuya, *Progress of Theoretical Physics* **16**, 45 (1956).
- <sup>15</sup> P. O. Gartland and B. J. Slagsvold, *Phys. Rev. B* **12**, 4047 (1975).
- <sup>16</sup> Y. Hasegawa and P. Avouris, *Phys. Rev. Lett.* **71**, 1071 (1993).
- <sup>17</sup> I. E. Tamm, *Phys. Z. Sowjet.* **1**, 733 (1932).
- <sup>18</sup> W. Shockley, *Phys. Rev.* **56**, 317 (1939).
- <sup>19</sup> S. G. Davison and M. Steslicka, *Basic Theory of Surface States* (Clarendon Press, 1996).
- <sup>20</sup> P. Heimann, J. Hermanson, H. Miosga, and H. Neddermeyer, *Phys. Rev. Lett.* **42**, 1782 (1979).
- <sup>21</sup> F. Reinert, G. Nicolay, S. Schmidt, and D. Ehm, S. Hüfner, *Phys. Rev. B* **63**, 115415 (2001).
- <sup>22</sup> A. Winkelmann, A. A. Ünal, C. Tusche, M. Ellguth, C.-T. Chiang, and J. Kirschner, *New Journal of Physics* **14**, 043009 (2012).
- <sup>23</sup> L. Bürgi, L. Petersen, H. Brune, and K. Kern, *Surface Science Letters* **447**, L157 (2000).
- <sup>24</sup> E. Simon, B. Újfalussy, B. Lazarovits, A. Szilva, L. Szunyogh, and G. M. Stocks, *Phys. Rev. B* **83**, 224416 (2011).
- <sup>25</sup> Paul N. Patrone, T. L. Einstein, *Phys. Rev. B* **85**, 045429 (2012).
- <sup>26</sup> M. Hyldgaard, Per Persson, *Journal of Physics: Condensed Matter* **12**, L13 (2000).
- <sup>27</sup> M. Ternes, A. J. Heinrich, and W. D. Schneider, *J. Phys.: Condens. Matter* **21**, 053001 (2009).
- <sup>28</sup> R. Requist, P. P. Baruselli, A. Smogunov, M. Fabrizio, S. Modesti, and E. Tosatti, *Nature Nanotechnology* **11**, 499 (2016).
- <sup>29</sup> H. Brune and P. Gambardella, *Surf. Sci.* **602**, 1812 (2009).
- <sup>30</sup> C. A. Büsser, G. B. Martins, and A. E. Feiguin, *Phys. Rev. B* **88**, 245113 (2013).
- <sup>31</sup> A. Allerdt, C. A. Büsser, G. B. Martins, and A. E. Feiguin, *Phys. Rev. B* **91**, 085101 (2015).
- <sup>32</sup> J. Li, W.-D. Schneider, R. Berndt, and B. Delley, *Phys. Rev. Lett.* **80**, 2893 (1998).
- <sup>33</sup> H. C. Manoharan, C. P. Lutz, and D. M. Eigler, *Nature* **403**, 512 (2000).
- <sup>34</sup> L. Limot and R. Berndt, *Appl. Surf. Sci.* **237**, 576 (2004).
- <sup>35</sup> M. A. Barral, A. M. Llois, and A. A. Aligia, *Phys. Rev. B* **70**, 035416 (2004).
- <sup>36</sup> N. Knorr, M. A. Schneider, L. Diekhöner, P. Wahl, and K. Kern, *Phys. Rev. Lett.* **88**, 096804 (2002).
- <sup>37</sup> R. Bulla, H.-J. Lee, N.-H. Tong, and M. Vojta, *Phys. Rev. B* **71**, 045122 (2005).
- <sup>38</sup> C.-Y. Lin, A. H. Castro Neto, and B. A. Jones, *Phys. Rev. B* **71**, 035417 (2005).
- <sup>39</sup> C.-Y. Lin, A. H. Castro Neto, and B. A. Jones, *Phys. Rev. Lett.* **97**, 156102 (2006).
- <sup>40</sup> M. A. Schneider, L. Vitali, N. Knorr, and K. Kern, *Phys. Rev. B* **65**, 121406 (2002).
- <sup>41</sup> Q. Li, S. Yamazaki, T. Eguchi, H. Kim, S. J. Kahng, J. F. Jia, Q. K. Xue, and Y. Hasegawa, *Phys. Rev. B* **80**, 115431 (2009).
- <sup>42</sup> S. S. Pershoguba and V. M. Yakovenko, *Phys. Rev. B* **86**, 075304 (2012).
- <sup>43</sup> W. A. Harrison, *Physica Scripta* **67**, 253 (2003).
- <sup>44</sup> G. A. Burdick, *Phys. Rev.* **129**, 138 (1963).
- <sup>45</sup> T. Shirakawa, S. Yunoki, *Phys. Rev. B* **90**, 195109 (2014).
- <sup>46</sup> K. G. Wilson, *Rev. Mod. Phys.* **47**, 773 (1975).
- <sup>47</sup> S. R. White, *Phys. Rev. Lett.* **69**, 2863 (1992).
- <sup>48</sup> S. R. White, *Phys. Rev. B* **48**, 10345 (1993).
- <sup>49</sup> F. A. Wolf, I. P. McCulloch, and U. Schollwöck, *Phys. Rev. B* **90**, 235131 (2014).
- <sup>50</sup> A. Allerdt, A. Feiguin, and S. D. Sarma, *Phys. Rev. B* **95**, 104402 (2017).